Development of a Data Acquisition System for a 3ω-Thermal Experiment

Matthew Oostman

Department of Physics

Oregon State University

June 28th, 2012

A report submitted to the Department of Physics in partial fulfillment of the requirements for the M.S. Physics (project option). The project was supervised by Prof. Janet Tate

ABSTRACT

A LabVIEW program to automate data collection in a thermal conductivity experiment is described, and preliminary measurements are reported using the new software. The system implements the "3ω method" to extract the thermal conductivity of a dielectric substrate at room temperature from the frequency-dependent third harmonic of the voltage across a thin-film heater deposited on the substrate. The program interfaces a lock-in amplifier, AC voltage source and a digital oscilloscope to a standard desktop computer via a GPIB interface. Preliminary measurements using Ag heaters on YSZ, fused SiO2, SrTiO3 and MgO yield reproducible data that give thermal conductivities that are systematically high compared to published values by about by 20% (SrTiO3), 50% (MgO), 200% (fused SiO2), but which are in the range of published data for YSZ.

INTRODUCTION & THEORY

The 3ω method is a technique by which the thermal conductivity of a material can be determined. A heater, usually a thin metal film, is placed in intimate thermal contact with a substrate and heated by an input of AC electrical power. Voltage oscillations across the heater are then measured and this data can be used to determine the thermal conductivity of the sample.

The premise of the 3ω method is described by D.G. Cahill[1-3] and expanded upon by others. [3-5] In the most basic implementation, a thin metal film is deposited upon a sample of interest and acts as both a heater and thermometer in the experiment. An AC current I with frequency ω is applied to the metal film. Because the temperature increase is proportional to the input of power P through the resistor R by $P = I^2R$ the resistance of the sample oscillates with temperature at a frequency 2ω, shown in figure 1. The resulting voltage oscillations $V = IR$ are then at a frequency 3ω.
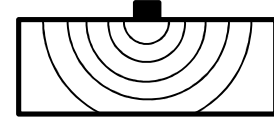

Figure 1: Thermal waves propagate into the sample at a frequency 2ω

The amount by which the metal film is heated is dependent on how quickly the heat diffuses through the sample and the thermal coefficient of resistance (TCR) of the heater α, so by measuring the thermal oscillations ΔT the thermal conductivity of the sample can be determined:

$$\Delta T = 2\frac{V_{3\omega}}{\alpha V_{1\omega}} \quad (1)$$

where

$$\alpha = \frac{1}{R}\frac{dR}{dT} \quad (2)$$

and where $V_{1\omega}$ and $V_{3\omega}$ are the root mean squared amplitude of the voltage across the sample at the fundamental and third harmonic, respectively.

The heat propagates primarily through the sample away from the metal film, even in air, which is a poor conductor of heat.[1] Other effects, such as the finite dimensions of the sample and heat reflections from the boundaries, can be accounted for with appropriate mathematical modeling.[4,5] The most straightforward model[6] calculates the temperature oscillations ΔT at a radial distance from the heater r by approximating the heater as a one-dimensional line with a length 2b on an infinitely thick substrate. The oscillations are a function of the 2ω power per unit length $\frac{P}{l}$, the thermal conductivity k, and a zeroth-order modified Bessel function K_0, which is in turn a function of the thermal diffusivity D. In this model, the temperature oscillations are given by: [6]

$$\Delta T(r) = \frac{P}{l\pi k}K_0\left(\sqrt{\frac{i2\omega}{D}}r\right) \quad (3)$$

In the limit where $\left(\sqrt{\frac{i2\omega}{D}}\,r\right) \ll 1$ and where $\sqrt{\frac{D}{i2\omega}} \gg b$ and assuming that there is no thermal boundary between the heater and the sample, it can be shown that this reduces to[1]

$$\Delta T = \frac{P}{l\pi k}\left(-\frac{1}{2}ln(\omega) - \frac{1}{2}ln\left(\frac{ib^2}{D}\right) + C\right) \quad (4)$$

where C is an integration constant. To show that this approximation is valid for this system, Corning 1737 glass has a diffusivity of 5.04×10^{-7} m²/s and a linear region in the in-phase voltage response near 1 Hz. Using these values $\sqrt{\frac{D}{i2\omega}} = 205\mu m$, which is significantly larger than the heater half-width of approximately 20 µm. Equation 4 has been arranged to separate the in- and out-of-phase components, where the in-phase component is real and scales with the natural logarithm of the frequency and the out-of-phase component is imaginary and is constant. It is in the regions where these approximations are true that this relationship holds and the thermal conductivity can be extracted from the slope of a plot of the temperature oscillations versus the natural log of the frequency.

APPARATUS

The apparatus contains: an input signal source, the circuitry, the sample itself, a lock-in amplifier (LIA), and a computer. Throughout the construction of the 3ω apparatus, the identity of the input signal
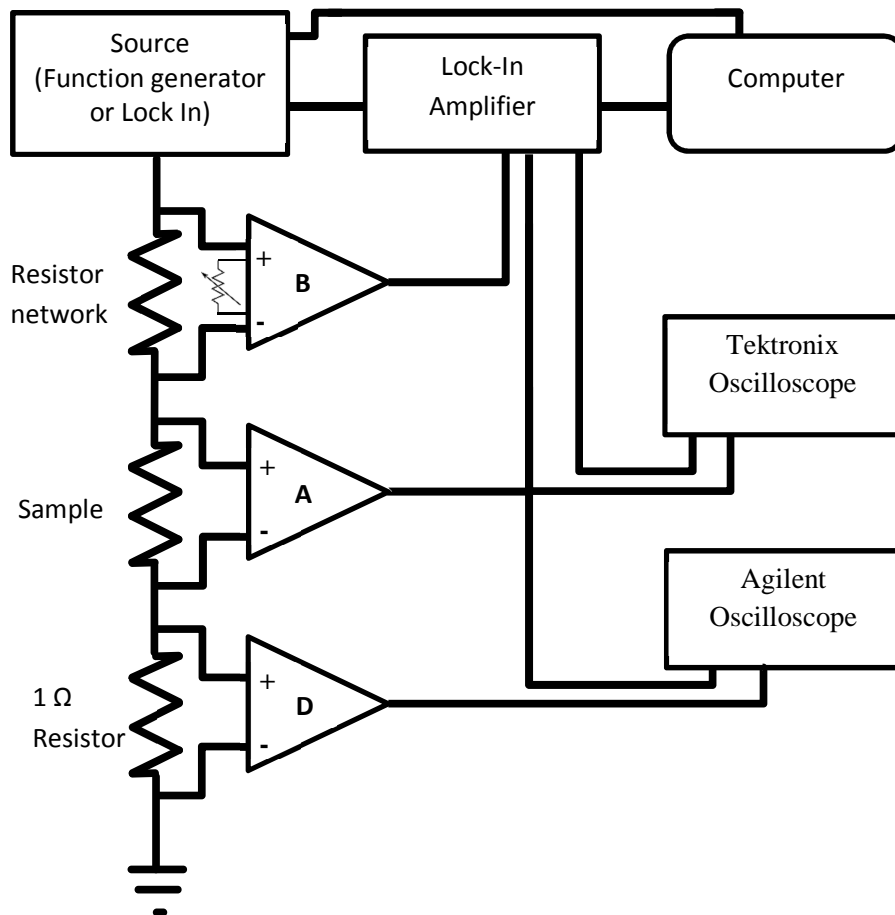

3

Figure 2: A basic schematic of the 3ω circuit. When the signal source is the LIA, the source block is omitted and all connections go through the LIA.

source has been revised several times. Initially, the source was a Stanford Research Systems SR850 LIA, the same lock-in as is used to detect the 3ω signal. The lock-in was initially abandoned as the signal source because it could only generate a signal at a maximum of 5 volts RMS. The following source was a Stanford Research Systems DS345 function generator. This was a promising source because it was capable of producing a more powerful signal with a maximum output of 10 volts RMS. Unfortunately, this source introduces a slight phase shift into our data, and after some troubleshooting, was abandoned. For most applications at this time, higher power isn't required to produce a detectable signal, so the original SR850 LIA was revisited. The system is currently designed to use either instrument at the option of the user, though all data presented herein use the lock-in as both the source and as the detector.

The circuitry composes a set of input and output ports, the sample holder, a set of differential amplifiers, an attenuating potentiometer, a thermally stable resistor network, a 1-ohm resistor, and a low-noise power supply as seen in figure 2. All of the circuitry is housed inside a grounded, metal case to help reduce the effects of noise.

The system is designed to take a single input signal at a user-determined frequency and voltage. This voltage drops across three series resistors: the sample, the resistor network, and the 1-ohm resistor. Each of these voltage drops are measured by unity-gain differential amplifiers.

A great deal of care and testing went into the selection of the amplifiers. Beyond the ability for the amplifiers to introduce noise, many of the amplifiers tested introduced significant phase shifts at high frequency. The experiment is quite sensitive to phase, selecting amplifiers with a minimum of phase shift was ideal, and all of the amplifiers are Texas Instruments INA128P precision, low power instrumentation amplifiers.

The signal from the sample and the resistor network (the A and B signals, respectively) are passed back to the LIA for comparison, while the signal from the 1-ohm resistor (the D signal) is passed to an Agilent Technologies InfiniiVision DSO-X 2002A digital oscilloscope and converted to a current reading. The signal across the sample is split off on its way to the LIA and also displayed on the Agilent oscilloscope to measure the 1ω voltage. This signal is further split to display the wave on a Tektronix 2205 oscilloscope alongside the difference between the A and B signals, which has been returned from the LIA.
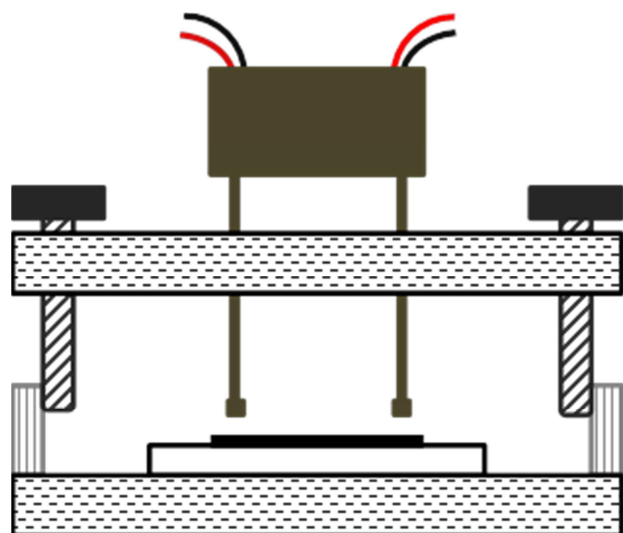

Figure 3: A side view of the sample holder. Each pogo pin shown has an adjacent neighbor. A four-probe measurement is used to eliminate contact resistance as an issue.

The resistor network exists to match the resistance of the sample so that a similar 1ω signal can be subtracted from the sample signal, allowing us to isolate the 3ω signal. The network consists of an assortment of low noise, thermally stable Ohmite resistors that can be connected in series in a variety of combinations to create an effective resistor with approximately the same net resistance as the sample. To fine tune the signal, a 450 kΩ 10-turn potentiometer is used adjust the gain of the amplifier so that the signals provided to the LIA are as closely matched as possible.

The sample holder depicted in figure 3 is designed to attempt to minimize potential contact issues and to provide repeatable results. The sample rests upon a small platform with posts at the corners to provide consistent spacing between the platform and the top of the holder. The top of the holder contains a set of four spring-mounted pogo pins with flat heads and a pair of thumb screws to hold the top in place. The pogo pins are set in pairs, approximately 2 mm between neighbors and 1 cm between pairs. When the top of the holder is screwed into place, the force from the pogo pins secures the sample and provides a consistent amount of pressure when taking measurements on substrates of equivalent thickness. Flat headed pogo pins are used because sharp points may puncture though thin films on the surface of the substrate.

SOFTWARE

Significant advancements have been made to the 3ω system by means of developing an automated method for the collection of data and setup and calibration of the instruments via a single user interface. This interface was designed in LabVIEW v10.0 and controls both the signal source as well as the detector, a LIA. The program is general enough and versatile enough to accommodate an assortment of sources and detectors. Without any alteration to the program, either a Stanford Research Systems SR850 or SR830 LIA can be used as the detector, dependent only upon which instrument is connected to the computer. A switch on the LabVIEW user interface chooses either a Stanford Research Systems DS345 function generator or the connected LIA as the signal source. The most up-to-date version of the program can be found on the COSINe research storage drive at: T:\physics\tate group\share\LabVIEW programs\3w (date).vi

The user enters a number of parameters essential to the data analysis, e.g. the measured 1ω voltage, the current in the circuit, and the dimensional and thermal properties of the heater, and may also enter comments. This information is saved with the voltage and frequency measurements and other settings obtained from the instruments in a single file.

The primary function of the program is to measure the voltage oscillations as a function of frequency. These data can then be used to determine the temperature oscillations with respect to frequency. The SR850 LIA, SR830 LIA, and the DS345 function generator are manufactured by Stanford Research Systems and share very similar commands and syntax. While this is primarily beneficial, the few differences that exist can be problematic. To make the transition between signal sources smooth for the user, all possible variations of commands and syntax are built into the program and only those that pertain to the user's chosen source are used.

The program progresses through several phases as depicted in figures 4 and 5: initialization, setup, the main data collection portion of the program, and compilation and documentation. Both the Initialization and Setup phases can be skipped at the user's option. Once the system has undergone the initialization process, the
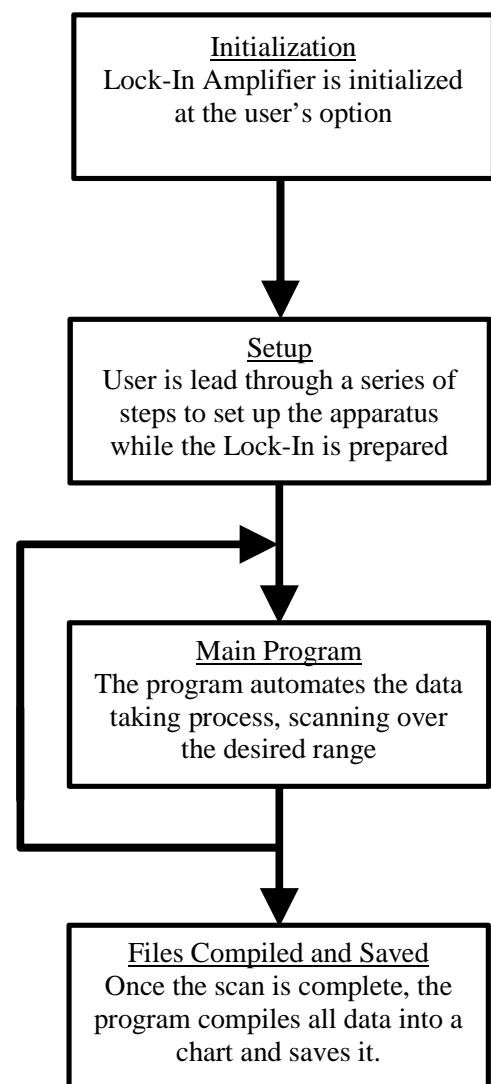

Figure 4: A basic outline of the 3ω program. More detailed descriptions of the Initialization, Setup, and Main portion of the program are included below.

system remains able to take data unless settings have been changed on the LIA or the system has been completely shut down, as in the case of prolonged disuse or a power outage. Setting up the system is usually necessary for each sample, though this step could be skipped if one was re-taking data or changing the range of data for a sample for which the system is already set up.

The initialization phase, described in figure 6, first resets the LIA to its factory default settings so that a consistent starting place is available and necessarily undoes any alterations to the lock-in that may be overlooked. It takes some time to complete this process, so after a delay of one minute the necessary settings are altered from the factory defaults to the settings used by the setup and measurement portions of the program. The primary undertaking of the initialization is to set various filters and ensure that a common reference point is established in case a measurement needs to be repeated on another occasion. The system is designed to have a shared ground for all components to reduce possible sources of noise, and the Lock-In can be directed to use this ground as well. The Offset and Expand functions have proven particularly troublesome in the past and were revealed to be the source of an error in spite of the fact that they hadn't been knowingly adjusted by any user, so to eliminate this problem they are reset to an Offset of 0.00% and an Expand of 1 for the X, Y, and R values for our measurements during the initialization phase.
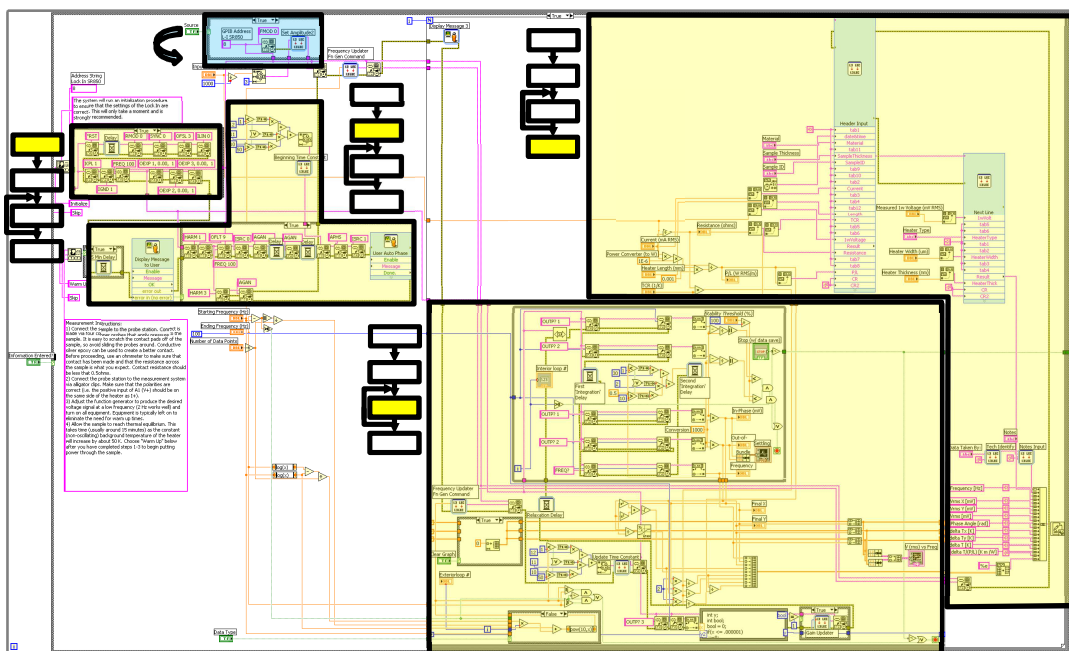

Figure 5: The various stages of the LabVIEW program are highlighted (in yellow) with an indication of what section they pertain to: initialization, setup, main, or compilation and recording. The section highlighted in blue and indicated by the twisted arrow switches between code as necessary to accommodate the differences between signal sources. Code not highlighted is communication with the user via text boxes between stages or basic math that is re-used in multiple areas.

Initialization

*RST
Resets the system to factory defaults

Delay

RMOD 0
Sets the Reserve Mode to Off

SYNC 0
Sets the Synchronous Filter to Off

OFSL 3
Sets the Low Pass Filter Slope to 24dB/oct

ILIN 0
Sets the Line Notch Filter to Out

ICPL 1
Sets the Input Coupling to DC

IGND 1
Sets the Input Shield Grounding to Ground

FREQ 100
Sets the Source to a frequency of 100 Hz

OEXP 1, 0.00, 1
Sets the X Offset to 0% and Expand to 1

OEXP 2, 0.00, 1
Sets the Y Offset to 0% and Expand to 1

OEXP 3, 0.00, 1
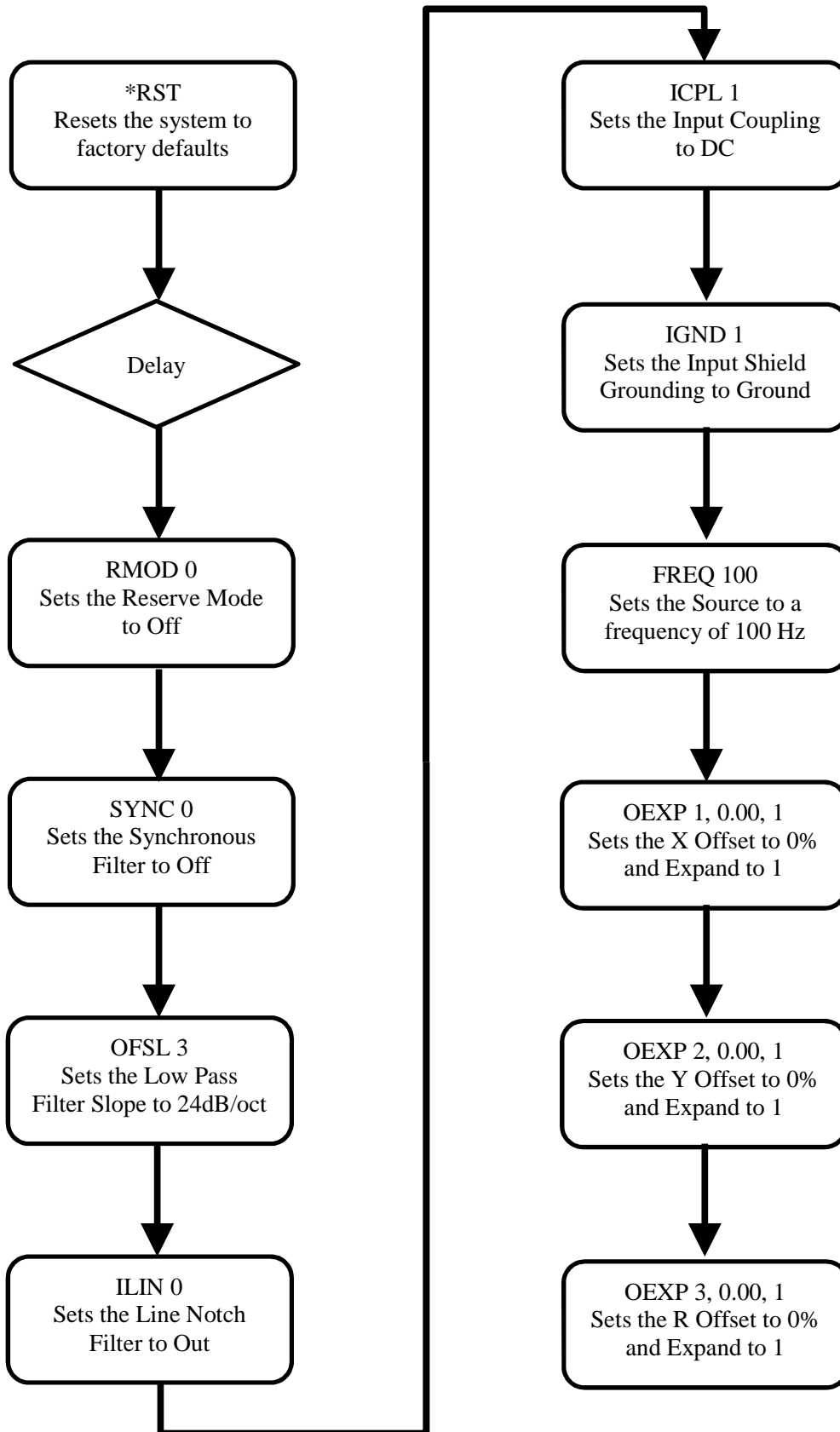Sets the R Offset to 0% and Expand to 1

Figure 6: The initialization phase of the LabVIEW program with the commands given to the LIA and signal source.

The setup phase, described in figure 7, is necessary for each new sample, as the individual parameters of the measurement will have changed. Essentially, the setup phase aligns the phase of the 1ω source signal and the sample signal (the A signal). This is best done at a moderate frequency, so after setting the Lock-In to watch the first harmonic at an appropriate time constant the source is instructed to produce a 100 Hz signal. Depending on the amplitude of the input signal, the system will then automatically adjust the sensitivity of the LIA so that it the best range is available. The auto-gain feature takes 10-30 seconds and has been frequently seen to miss the optimum range on its initial pass, especially in cases where the previous setting is far from the current best setting, as in the case where the system has just been used to take data in a much higher or lower range. To alleviate this issue, the auto-gain function is run a second time.

After the optimum gain setting is found, the system increases the time constant to improve the accuracy of the following adjustments. The LIA is instructed to look at the difference in the A and B signals, from the sample and the resistor network respectively, and told to adjust the phase until the entire signal is in-phase and there is no out-of-phase component. The system utilizes the LIA's auto-phase feature to do this. This feature takes a widely variable amount of time to complete, and like the auto-gain feature, does not always find the optimum setting on the first try. Because this occasionally takes four or more attempts, it is left to the determination of the user to decide when the phase has been properly aligned and to repeat the auto-phase procedure until they are satisfied.

Once the phase procedure has been completed, the LIA is set to listen to the third harmonic. The 3ω signal is considerably weaker so the sensitivity of the LIA must be adjusted again. The auto gain procedure is run again and then the system is ready to take data.

In its most basic form, the main portion of the program, seen in figure 8, reads the in-phase and out-of-phase components of the 3ω voltage from the LIA then waits a short time, typically 0.5-5 seconds, and re-takes those same measurements. If the first and second readings are stable within the desired error, the program records the most recent values as well as the frequency at which those measurements were taken.

The error is determined by the user as a percentage difference between two consecutive readings. Due to noise, no two readings will ever match perfectly, and so it is left to the user to decide when the value has settled enough. The computer compares the readings using the following equation:

$$\left| \frac{first\ reading - second\ reading}{second\ reading} \right| \times 100\% \leq user\ defined\ stability \quad (5)$$

The program waits at a single frequency, continuously taking readings, until both the in-phase and out-of-phase readings have met this condition. Typically, the stability threshold can be set quite low, less than one percent, though increased precision comes at a cost of progressively longer wait times. Because the entire process has been automated, the stability threshold has been placed near the extreme end of the possible range at 0.05% for all measurements presented herein. It is possible to collect data at slightly lower tolerance on some substrates, but no substrate tested was stable within 0.01% over the entire frequency range, so 0.05% was chosen as the most practical range.
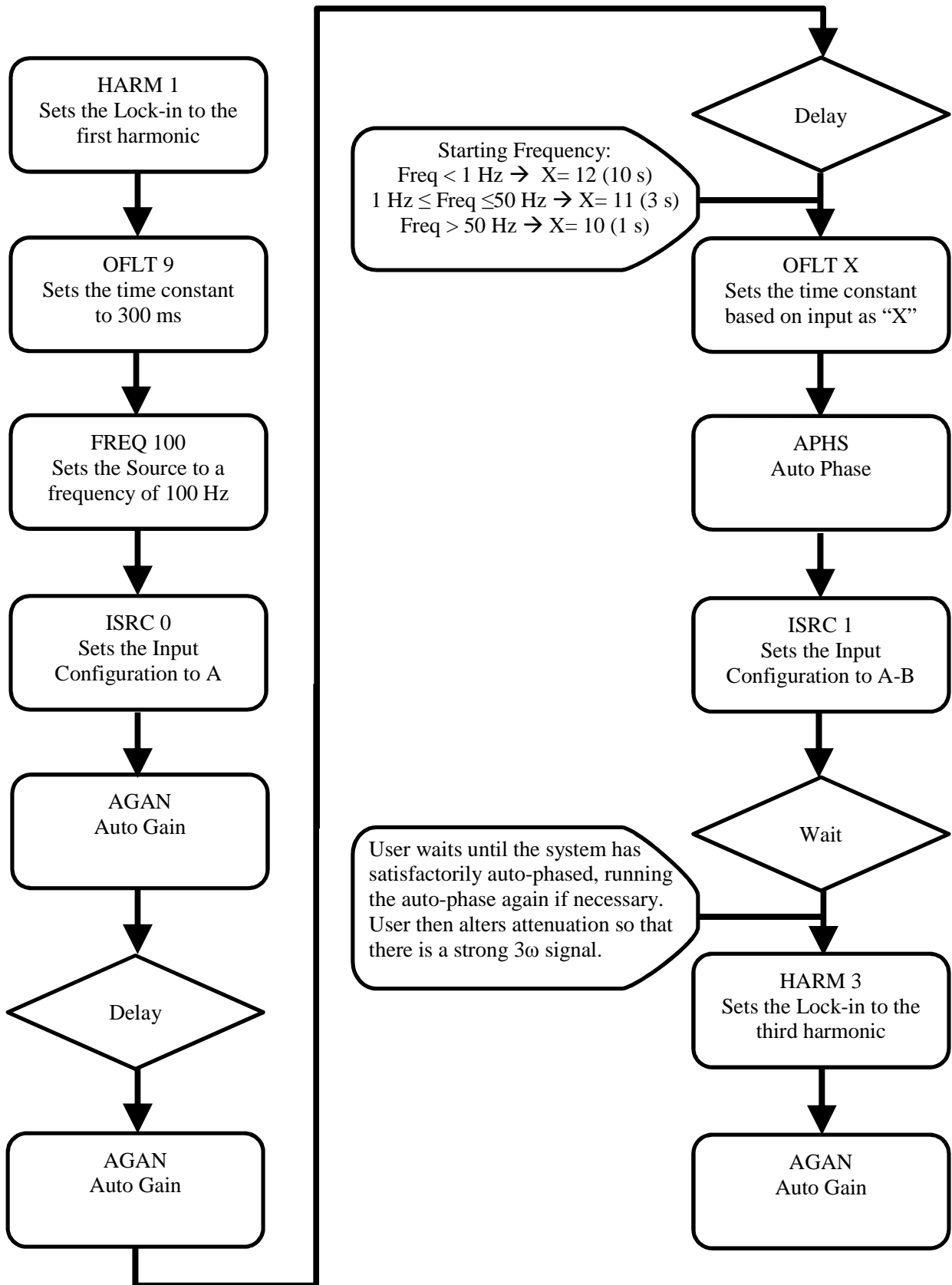
Setup

HARM 1
Sets the Lock-in to the first harmonic

OFLT 9
Sets the time constant to 300 ms

FREQ 100
Sets the Source to a frequency of 100 Hz

ISRC 0
Sets the Input Configuration to A

AGAN
Auto Gain

Delay

AGAN
Auto Gain

Starting Frequency:
Freq < 1 Hz → X= 12 (10 s)
1 Hz ≤ Freq ≤50 Hz → X= 11 (3 s)
Freq > 50 Hz → X= 10 (1 s)

Delay

OFLT X
Sets the time constant based on input as "X"

APHS
Auto Phase

ISRC 1
Sets the Input Configuration to A-B

Wait

User waits until the system has satisfactorily auto-phased, running the auto-phase again if necessary. User then alters attenuation so that there is a strong 3ω signal.

HARM 3
Sets the Lock-in to the third harmonic

AGAN
Auto Gain

Figure 7: The setup phase of the LabVIEW program with the commands given to the LIA and signal source.

At every measurement the GPIB Read buffer is cleared at the computer. While this step has not always been necessary, the buffer occasionally fills up, causing delayed responses to queries to the LIA. This in turn causes the program to record successive readings out of order and as nonsensical responses to mundane queries. Clearing the GPIB buffer regularly eliminates these issues but requires that the entire program communicate exclusively using GPIB protocol as intermixing GPIB and VISA protocol has been found to introduce these buffering errors even when the CLEAR command is used.

Once a stable measurement has been made, other useful information is derived from it, including the total magnitude of the 3ω voltage (R), the phase angle, the in- and out-of-phase temperature oscillations, the total magnitude of the temperature oscillations, and the temperature oscillations divided by the power per length of the heater. All of this information is compiled for each frequency step and is reported in a tab delineated text format for further analysis.

The size of the 3ω voltage and the range of interesting frequencies travel through several orders of magnitude and vary between samples, so the program is designed to alter the gain settings of the LIA between measurements at different frequencies to ensure the best possible sensitivity of the instrument and to prevent the LIA from becoming swamped. It is important that the range of the sensitivity is always slightly larger than either the in- or out-of-phase component; otherwise the LIA will report a value that is simply the top of the sensitivity range. Using the total magnitude of the signal (R) as the highest possible reading at this step, a simple C program (see Appendix II) is executed to determine the optimum gain setting. This ensures that no component of the signal will swamp the lock-in and that the readings will always be accurate without having to wait for the system to go through the auto-gain process at each step.

The slope of the ln(frequency) versus in-phase 3ω voltage plot determines thermal conductivity, so the program is designed to take data points in even increments in log space based on a user-defined frequency range and number of desired data points. Each time a stable reading has been recorded, the system steps to the next point f_{new} by incrementing to the next point given by:

$$f_{new} = 10^{\left(\left(\frac{\log(f_{end} - f_{start})}{n}\right) \times m + \log(f_{start})\right)} \quad (6)$$

where f_{start} and f_{end} are the user-defined starting and ending frequencies, n is the user-defined total number of data points the user desires, and m is a loop iteration integer, beginning at zero. Once the program has stepped to the newest frequency point, it assesses whether this point is above or below the desired range (because the program can run either up or down in frequency). The program continues taking data if f_{new} is within the user's range and if it is not, it ends the loop and saves the data as a tab delineated unformatted data file which can be opened as either a text file or as a spreadsheet.
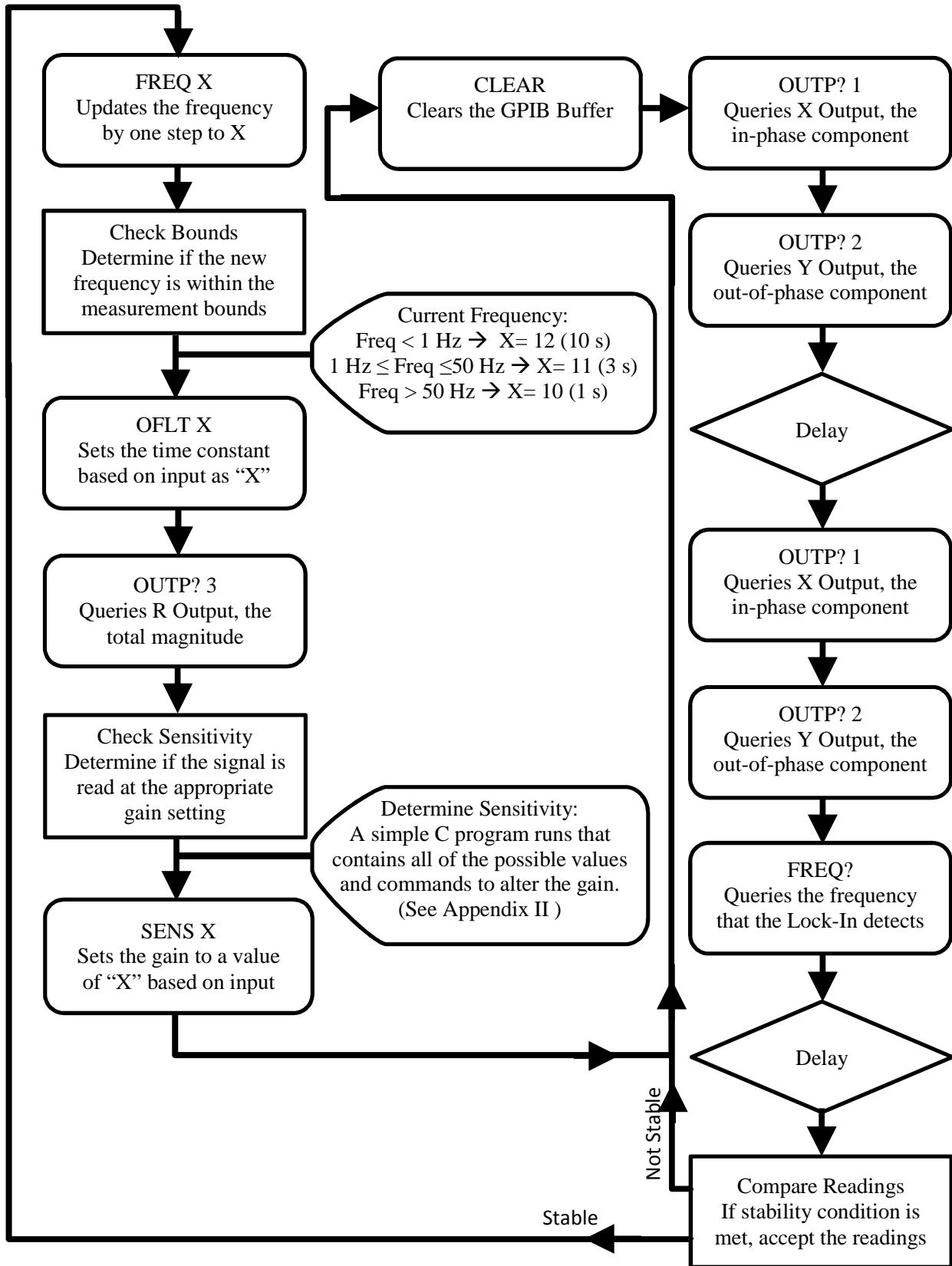
Main Program

Figure 8: The main phase of the LabVIEW program with the commands given to the LIA and signal source.

12

HEATERS

In this experiment, thin film silver lines act as both heaters and thermometers. The properties of these heaters must be well understood in order to interpret the results of the 3ω data properly. All of the heaters presented here are made of silver, though aluminum and platinum are also good potential heater materials. The bulk TCR is a quantity which characterizes the change in resistance of the heater with temperature. The relationship between resistance R and temperature T is described by[6]

$$R = R_0\big(1 + \alpha(T - T_0)\big) \quad (7)$$

where R_0 and T_0 are some base resistance and temperature, respectively. The heaters presented here are made of silver, which has a bulk TCR of 0.0038 K^{-1}.[6]

Heaters for the experiment are thin film metallic lines with a thickness t of approximately 150 nm, as seen in figure 9. Each heater has a width $2b$ that is approximately 20-50 microns with larger contact pads located at the ends. The length l of each heater presented here is 8 mm. The width varies on the order of 1-2 microns along the length of the heater, as illustrated by optical microscopy and seen in figure 10.
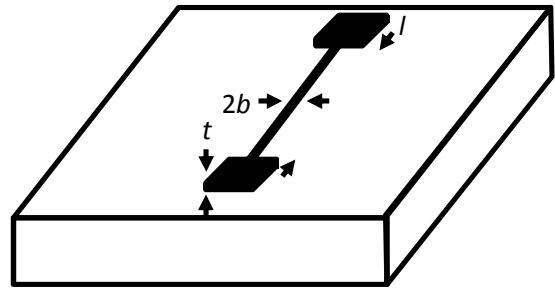

Figure 9: The thickness t, width $2b$, and length l of our heaters. Samples are generally 1-4 cm squares.

While the specific geometries of each sample are different, each sample is a substrate between 1 and 4 centimeters square with a thin heater placed generally near the center. In all of the samples studied for this project the silver heaters were deposited onto the substrates by thermal evaporation. Substrates are cleaned by sonication first in acetone, then isopropyl alcohol, then deionized water before deposition. A variety of shadow masks were made with various width heaters and used during thermal evaporation.
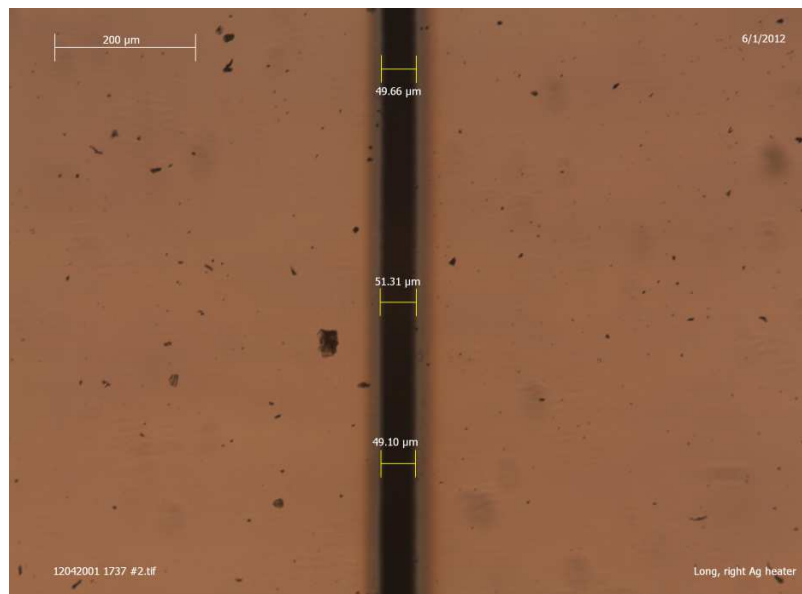
Attempts were made to improve the adhesion of the

Figure 10: Silver heater 50 µm ± 1.5 µm wide on Corning 1737 glass. The shadow effect around the heater is due to poor contact between the mask and substrate during deposition.

silver heaters by heating the substrates during deposition. Improving the adhesion of the heaters is important because the heaters must be in good thermal contact with the samples, otherwise an additional thermal barrier must be accounted for.

DATA

The frequency range in which the necessary approximations for using this method are valid vary by substrate due to their differing diffusivity. In figures 11 and 12 this range is approximately between 0.5-5 Hz, while in figures 13 and 14 the range is approximately 50-500 Hz. In this region ΔT_{ac} is constant with frequency for the out-of-phase component of the data and the in-phase data is linear with a negative slope.

Outside of this range the temperature oscillations no longer conform to this behavior. In the case of the 1737 glass in figure 12, the linear region is between 0.5 and 5 Hz. Above 5 Hz the out-of-phase region is no longer flat as should be expected, as the approximation that $\sqrt{\frac{D}{i2\omega}} \gg b$ is no longer valid, since $\sqrt{\frac{D}{i2\omega}} \approx 90$ µm and b =25 µm. At higher frequency

Figure 11 (above): ΔT vs. frequency for YSZ on a thick 2.8 mm (thick) substrate and a 1 mm (thin) substrate. Filled points indicate in-phase components while hollow points indicate out-of-phase components. Blue circles: thick substrate with a 28.1 µm heater; red squares: thick substrate with a 35 µm heater; green triangles: thin substrate with a 45.1 µm heater.

Figure 12 (below): ΔT vs. frequency for a 1 mm Corning 1737 glass substrate. Filled points indicate in-phase components while hollow points indicate out-of-phase components. Blue circles: 35.7 µm heater; red squares: 50 µm heater.

the wavelength of the thermal oscillations approach the order of the width of the heater, invalidating the approximation that the heater is a 1-dimentional line. In the low frequency limit the wavelength of
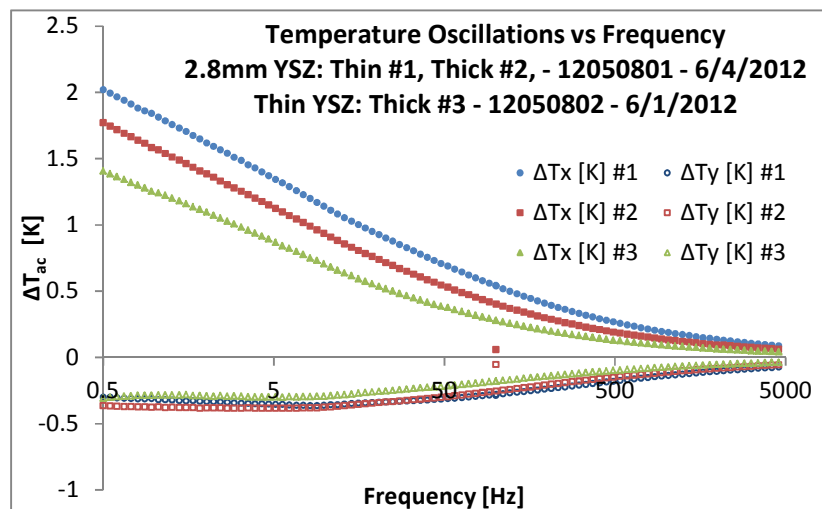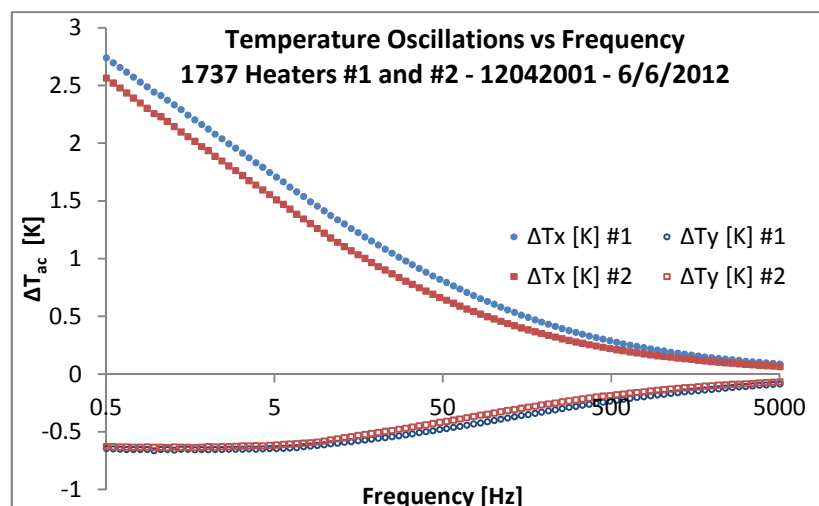
the thermal oscillations are long and the approximation that the substrate is very large relative to the oscillations no longer holds.

Data have been collected for a variety of substrate materials and the results plotted in figures 11-14. For yttria stabilized zirconia (YSZ) two different samples are presented in figure 11; all other plots are for single substrates. For each material the thermal conductivity has been determined from the slope of the ΔT_{ac} versus ln(frequency) plot and compiled in figure 15.

The thermal conductivity for YSZ and for 1737 glass is consistent between heaters, while the thermal conductivity for $SrTiO_3$ varies a bit more. Only one MgO heater gave sensible results, the other heater may have burned out.

The measurement of YSZ yields a thermal conductivity of approximately 2.8 W/(m K) across all heaters' widths and substrate thicknesses which is very close to the literature reported range of 2.2-2.9 W/(m K).[7] The measured thermal conductivity of $SrTiO_3$ is 12.9-15.9 W/(m K) which is about 30% higher than the literature value of 11.2 W/(m K).[10] Thermal conductivity measurements of 1737 are also consistently high, though are also fairly precise at 1.9 W/(m K)
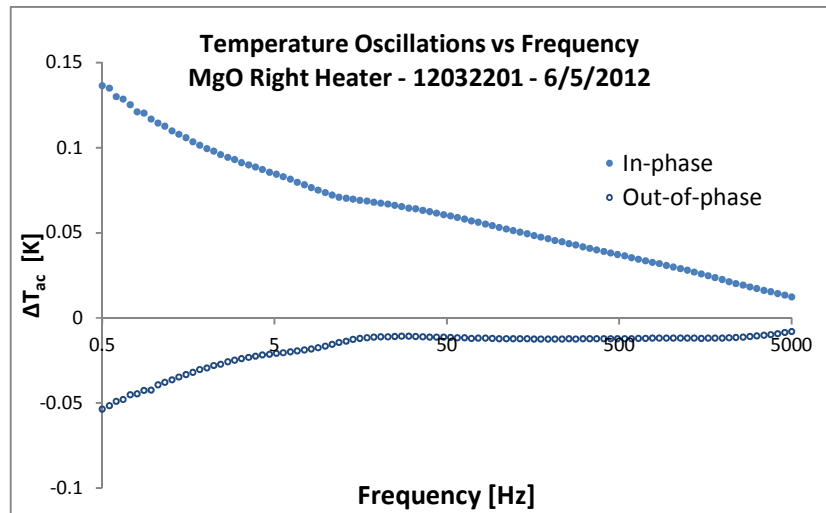

Figure 13 (above): ΔT vs. frequency for a 1 mm MgO substrate with an Ag heater. Filled points indicate in-phase components while hollow points indicate out-of-phase components. The heater is 26.1 µm wide.

Figure 14 (below): ΔT vs. frequency for a 1 mm $SrTiO_3$ substrate. Filled points indicate in-phase components while hollow points indicate out-of-phase components. Blue circles: 32 µm heater; red squares: 35.3 µm heater.
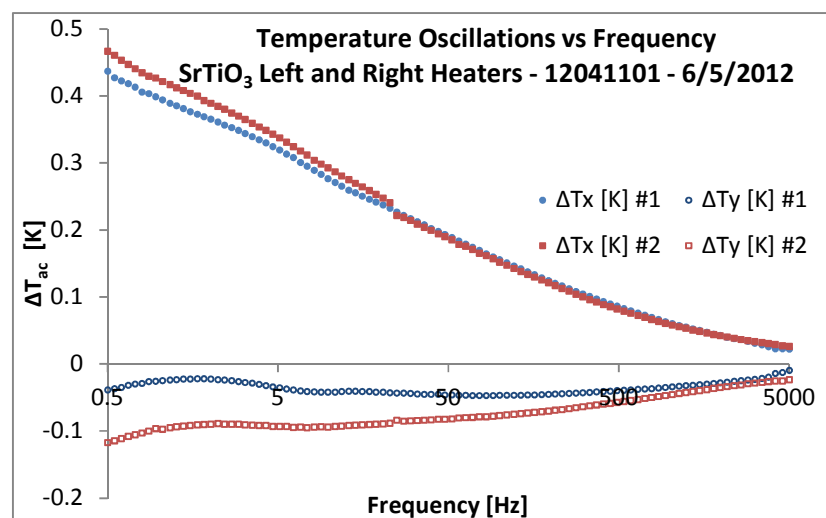
which is approximately twice the literature reported value of 0.91 W/(m K).[8] The thermal conductivity of MgO is similarly high at 85 W/(m K); the literature value varies from 45-60 W/(m K).[9]

While the thermal conductivity values that have been determined by the 3ω method are for the most part inaccurate, the consistency of most results are quite promising and seem to indicate a systemic issue. Likely causes include insufficient characterization of the heaters, particularly that the TCR of the thin film heaters may not be the same as the TCR of bulk silver, and poor adhesion between the heater and the sample, which introduces an additional thermal boundary that is otherwise unaccounted for.

	Heater width [microns]	I [mA rms]	V1w [mV rms]	R [ohms]	P/l [W/m rms]	TC [W/m K]	Literature TC [W/m K]
Thick YSZ Left Heater - 12050801 - 6/4/2012	28.1	47	915	19.47	5.38	2.84	2.2-2.9[7]
Thick YSZ Right Heater - 12050801 - 6/4/2012	35	51	770	15.1	4.91	2.79	2.2-2.9[7]
Thin YSZ Left Heater - 12050802 - 6/1/2012	45.1	54	652	12.1	4.40	2.85	2.2-2.9[7]
1737 Heater #1 - 12042001 - 6/6/2012	35.7	35	1260	36	5.51	1.98	0.91[8]
1737 Heater #2 - 12042001 - 6/6/2012	50	45	965	21.4	5.43	1.93	0.91[8]
MgO Right Heater - 12032201 - 6/5/2012	26.1	43	1000	23.3	5.38	85.13	45-60[9]
SrTiO$_3$ Left Heater - 12041101 - 6/5/2012	32	37	1060	28.7	4.90	15.90	11.2[10]
SrTiO$_3$ Right Heater - 12041101 - 6/5/2012	35.3	43	1000	23.3	5.38	12.94	11.2[10]

Figure 15: Samples of different materials, heater widths, and measurement parameters. The thermal conductivity from each measurement is reported alongside a literature value for the thermal conductivity.

FUTURE WORK

As the system is currently designed, the user is able to run experiments that determine the thermal conductivity of bulk dielectrics. With very little modification to the programing and sample preparation, the system could be set up to measure the thermal conductivity of thin films. As was briefly discussed earlier, poor thermal contact between the heater and the substrate introduces an additional thermal boundary that could be accounted for with computational modeling. This same technique could be used to characterize the thermal boundary should one be introduced on purpose, as in the case of a thin film.

In the limit that the thickness of the film is much smaller than the width of the heater and the thermal conductivity of the film is small compared to the thermal conductivity of the substrate, the film acts as a small thermal barrier,[3] such that:

$$\Delta T_{total} = \Delta T_{substrate} + \Delta T_{film} \quad (8)$$

Under our assumptions, ΔT_{film} is a frequency-independent quantity given by:[2]

$$\Delta T_{film} = \frac{Pt}{2blk_{film}} \quad (9)$$

Using this information, one might use a well characterized substrate and heater deposition method to deposit two identical heaters upon the same substrate. By placing one heater in a region without a film and the other in a region with a film the 3ω technique could be used to determine the difference in ΔT_{total}, thereby extracting ΔT_{film}.

Similarly, this technique could be used in conjunction with two heaters of different width upon a substrate with a uniform film across its entirety. The difference between the two measurements of ΔT_{total} can then be attributed to the difference in ΔT_{film}. Because ΔT_{film} is dependent on the heater width, the total dependence of both measurements on ΔT_{film} versus heater width can be extracted.

By using either method described above to determine ΔT_{film} the thermal conductivity of the film can be known. These methods are highly dependent on the assumptions and approximations made, as well as very well-known substrate, heater, and film properties. However, in the region where these approximations are valid and the dimensionality of the components can be well established, this method provides a relatively simple method for establishing the thermal conductivity of novel thin film materials.

CONCLUSIONS

A software program has been developed for control of an apparatus which has been built to measure the thermal conductivity of materials. The system utilizes the 3ω method to measure the thermal conductivity of YSZ, Corning 1737 glass, MgO, and SrTiO$_3$. The system yields reproducible and reasonably precise results with a standard deviation of approximately 2%, whose accuracy can be improved by future characterization of the heaters and advances to the apparatus.

<u>References</u>

[1] Cahill, David G. "Thermal Conductivity Measurement from 30 to 750 K: The 3ω Method." *Review of Scientific Instruments* 61.2 (1990): 802. Print.

[2] Cahill, David G., M. Katiyar, and J. R. Abelson. "Thermal Conductivity of A-Si:H Thin Films." *Physical Review B* 50.9 (1994): 6077-081. Print.

[3] Lee, S. -M, and D. G. Cahill. "Heat Transport in Thin Dielectric Films." *Journal of Applied Physics* 81 (1997): 2590. Print.

[4] Borca-Tasciuc, T., A. R. Kumar, and G. Chen. "Data Reduction in 3ω Method for Thin-film Thermal Conductivity Determination." *Review of Scientific Instruments* 72.4 (2001): 2139. Print.

[5] Jacquot, A., F. Vollmer, B. Bayer, M. Jaegle, D. G. Ebling, and H. Böttner. "Thermal Conductivity Measurements on Challenging Samples by the 3 Omega Method." *Journal of Electronic Materials* 39.9 (2010): 1621-626. Print.

[6] Carslaw, H. S., and J. C. Jaeger. *Conduction of Heat in Solids,*. Oxford: Clarendon, 1959. 195. Print.

[7] Nicholls, Lawson, and Johnstone. "Methods to Reduce the Thermal Conductivity of EB-PVD TBCs." *SURFACE & COATINGS TECHNOLOGY* 151 (2002): 383-91. Print.

[8] *Corning 1737 AMLCD Glass Substrates*. Tech. Corning, 2003. Web. <http://www.vinkarola.com/pdf/Corning%20Glass%201737%20Properties.pdf>.

[9] "Application of Magnesium Compounds to Insulating Heat-conductive Fillers." Web. 28 June 2012. <http://www.konoshima.co.jp/en/resdev/004.html>.

[10] "SrTiO3,LaAlO3, MgO Crystal Substrates, SrTiO3 LaAlO3 MgO Crystals, SrTiO3 Crystal Substrates, LaAlO3 Substrates." Web. 28 June 2012. <http://www.toplent.com/SrTiO3.htm>.

Appendix I:
User Interface

The LabVIEW program contains a graphical user interface for the data collection software depicted in figure 16. All of the information about the sample is logged on the left and all of the input controls and measurement parameters are in the central area. The user can select either the SR850 LIA (default) or the DS345 function generator as the signal source and to take data in either equal log steps (default) or equal linear steps. All of the text entries default to "Not Entered" and all numerical entries default to zero so that there is never a question of whether a value is correct or simply not entered when the data is reviewed. The notes section will accept up to 1000 characters and is often used to indicate which heater is being used on a multi-heater sample. The time and date of every measurement are recorded automatically.

The graph on the right hand side will actively display data as it is taken. The entries just below that for Frequency, In-Phase, and Out-of-Phase indicate the values of the most recent data point taken. The Clear button will remove all data from the graph without altering the actual data, though it will wait to remove data from the graph until it has new data to replace it with. The section in the bottom left gives the user a sense of how quickly each measurement is stabalizing. The lower graph plots 3ω voltage oscillations versus the total number of loops the program has iterated. Exterior loop number indicates which total data point the program is on, and Interior loop number indicates how many times the system has compared two consecutive values while determining if the voltage reading has stabilized.
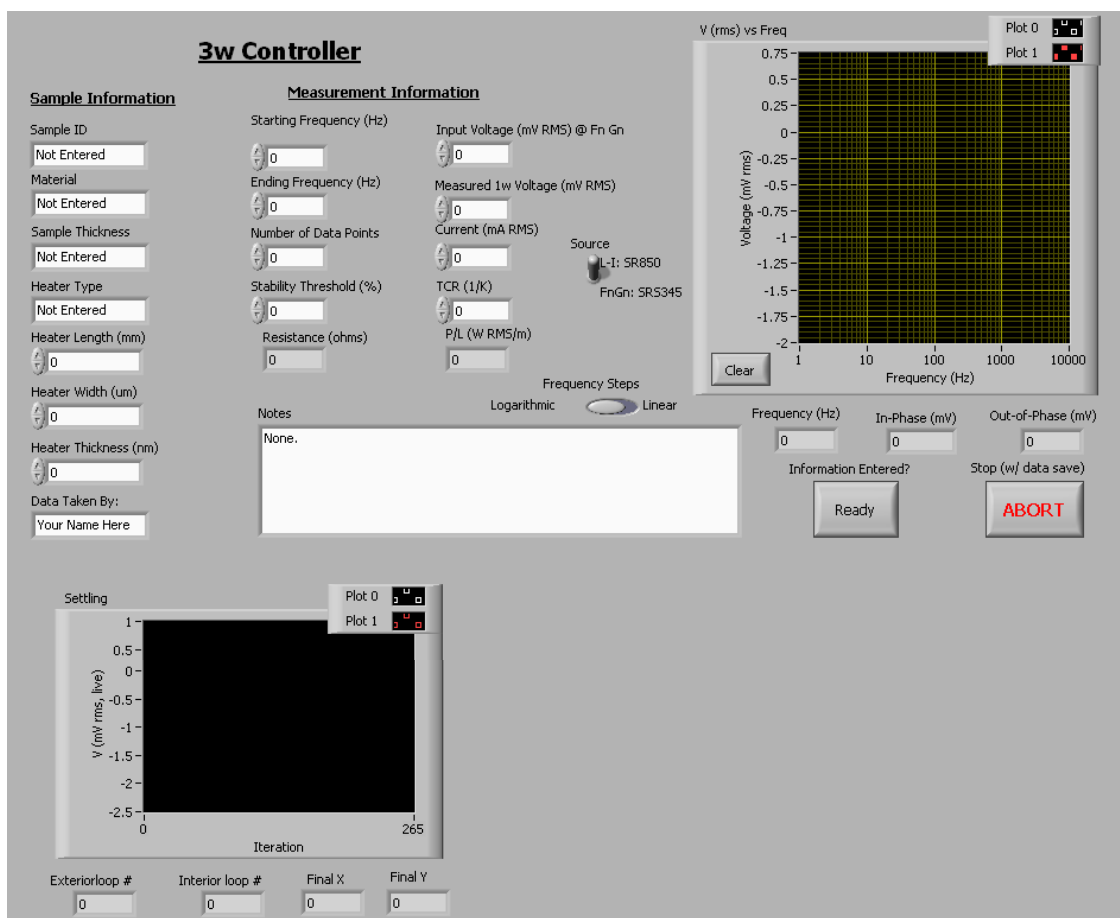
Figure 16: The user interface of the 3ω LabVIEW program. The "Settling" section in the bottom left isn't pertinent to every user, so it normally appears off of the screen.

Appendix II:
Programming

The LabVIEW program calls a simple C program at one step to determine what the appropriate gain setting should be. The SR850 LIA has a series of sequential numerical codes for the gain settings that step in uneven amounts, so it was significantly easier to write a short code that determined the correct setting and passed the corresponding code to the LabVIEW program than to program LabVIEW to make the judgment on its own. In this code, the input "x" is the value of the magnitude of the signal (R), the input "y2" is the existing gain setting, "y" is the new gain setting determined by the program (which becomes "y2" the next time the program is run), and "bool" is an integer value of 0 or 1 which is only set to 1 if the value does not change, which the LabVIEW program uses to determine if sending a new gain setting is necessary. The code is as follows:

```
int y;
int bool;
bool = 0;
if(x <= .000001)
 y=8;
if(x > .000001 && x <=.000002)
 y=9;
if(x > .000002 && x <=.000005)
 y=10;
if(x > .000005 && x <=.00001)
 y=11;
if(x > .00001 && x <=.00002)
 y=12;
if(x > .00002 && x <=.00005)
 y=13;
if(x > .00005 && x <=.0001)
 y=14;
if(x > .0001 && x <=.0002)
 y=15;
if(x > .0002 && x <=.0005)
 y=16;
if(x > .0005 && x <=.001)
 y=17;
if(x > .001 && x <=.002)
 y=18;
if(x > .002 && x <=.005)
 y=19;
if(x > .005 && x <=.01)
 y=20;
if(x > .01 && x <=.02)
 y=21;
if(x > .02 && x <=.05)
 y=22;
if(x > .05 && x <=.1)
 y=23;
if(x > .1 && x <=.2)
 y=24;
if(x > .2 && x <=.5)
 y=25;
if(x > .5 && x <=1)
 y=26;
if(y==y2)
 bool = 1;
```

Appendix III:
Data

Here I present a copy of a report that the 3ω system generates upon completion of its run.

```
Sample ID: 12042001                              Scan Date/Time: 6/6/2012 12:38:51 PM
Sample Material: 1737                            Sample Thickness: No Film

Measurement Parameters:
Current  [mA]: 45.000000          Length  [mm]: 8.000000
Voltage (1w) [mV]: 4000.000000    TCR [1/K]: 0.003800
Resistance [ohm]: 21.444444       Power per Length[W/m]: 5.428125

Measured 1w Voltage: 965.000000   Heater Material: Ag    Heater Width: 50.000000    Heater Thickness: 150.000000

Measurement Taken By: MO
Notes: Large heater, #2 per optical measurements
```

Frequency [Hz]	Vrms X [mV]	Vrms Y [mV]	Vrms [mV]	Phase Angle [rad]	delta Tx [K]	delta Ty [K]	delta T [K]	delta T/(P/L) [K]
5.000000E+03	1.251110E-01	-1.181370E-01	1.720730E-01	-7.567357E-01	3.070627E+00	-2.899463E+00	4.223226E+00	5.656848E-01
4.555800E+03	1.333830E-01	-1.202050E-01	1.807210E-01	-7.487751E-01	3.249106E+00	-3.194030E+00	4.435498E+00	5.986878E-01
4.151000E+03	1.382840E-01	-1.291120E-01	1.891887E-01	-7.511104E-01	3.393935E+00	-3.168823E+00	4.643301E+00	6.252508E-01
3.782300E+03	1.460620E-01	-1.342600E-01	1.983932E-01	-7.433214E-01	3.584832E+00	-3.295173E+00	4.869208E+00	6.604182E-01
3.446300E+03	1.532000E-01	-1.405410E-01	2.078090E-01	-7.432900E-01	3.760022E+00	-3.493329E+00	5.102513E+00	6.926926E-01
3.140100E+03	1.610080E-01	-1.464050E-01	2.176189E-01	-7.379310E-01	3.951655E+00	-3.592251E+00	5.341070E+00	7.279964E-01
2.861100E+03	1.690400E-01	-1.526780E-01	2.277830E-01	-7.345837E-01	4.148786E+00	-3.747210E+00	5.590529E+00	7.643130E-01
2.607000E+03	1.774140E-01	-1.591140E-01	2.385132E-01	-7.320092E-01	4.354311E+00	-3.912533E+00	5.853883E+00	8.021760E-01
2.375400E+03	1.861760E-01	-1.660300E-01	2.494543E-01	-7.282609E-01	4.569559E+00	-4.091116E+00	6.124114E+00	8.417938E-01
2.164300E+03	1.953250E-01	-1.733110E-01	2.611427E-01	-7.250088E-01	4.793905E+00	-4.254101E+00	6.409283E+00	8.831604E-01
1.972100E+03	2.047430E-01	-1.809010E-01	2.732121E-01	-7.236509E-01	5.025053E+00	-4.438994E+00	6.705506E+00	9.270433E-01
1.796900E+03	2.146070E-01	-1.887990E-01	2.858343E-01	-7.215100E-01	5.267148E+00	-4.637365E+00	7.015294E+00	9.703438E-01
1.637200E+03	2.251870E-01	-1.969640E-01	2.991722E-01	-7.186423E-01	5.526815E+00	-4.834131E+00	7.342650E+00	1.018181E+00
1.491800E+03	2.359460E-01	-2.053990E-01	3.128247E-01	-7.162949E-01	5.790875E+00	-5.041154E+00	7.677256E+00	1.066828E+00
1.359200E+03	2.470930E-01	-2.141010E-01	3.269468E-01	-7.139838E-01	6.064459E+00	-5.254729E+00	8.024328E+00	1.117229E+00
1.238500E+03	2.590140E-01	-2.233690E-01	3.420263E-01	-7.116387E-01	6.357038E+00	-5.482195E+00	8.394427E+00	1.171130E+00
1.128500E+03	2.714120E-01	-2.328170E-01	3.575867E-01	-7.090045E-01	6.661325E+00	-5.714080E+00	8.776330E+00	1.227831E+00
1.028200E+03	2.842560E-01	-2.426810E-01	3.737587E-01	-7.066119E-01	6.976588E+00	-5.956174E+00	9.173442E+00	1.285261E+00
9.369000E+02	2.979950E-01	-2.528450E-01	3.908089E-01	-7.036153E-01	7.313758E+00	-6.205631E+00	9.591711E+00	1.343828E+00
8.536700E+02	3.121510E-01	-2.631560E-01	4.082760E-01	-7.004399E-01	7.661192E+00	-6.456694E+00	1.002041E+01	1.411388E+00
7.778300E+02	3.269630E-01	-2.743320E-01	4.268054E-01	-6.980919E-01	8.024726E+00	-6.732992E+00	1.047518E+01	1.478361E+00
7.087300E+02	3.424900E-01	-2.856680E-01	4.459343E-01	-6.950133E-01	8.405809E+00	-7.008759E+00	1.094442E+01	1.548556E+00
6.457700E+02	3.587620E-01	-2.974290E-01	4.660195E-01	-6.922007E-01	8.805176E+00	-7.299866E+00	1.143762E+01	1.622139E+00
5.884000E+02	3.756010E-01	-3.094690E-01	4.866699E-01	-6.891632E-01	9.218459E+00	-7.595367E+00	1.194444E+01	1.698277E+00
5.361300E+02	3.933330E-01	-3.219270E-01	5.082930E-01	-6.858995E-01	9.653605E+00	-7.901126E+00	1.247481E+01	1.778452E+00
4.885000E+02	4.117210E-01	-3.346220E-01	5.305526E-01	-6.824609E-01	1.010496E+01	-8.212702E+00	1.302147E+01	1.861593E+00
4.451000E+02	4.311820E-01	-3.478550E-01	5.540045E-01	-6.788418E-01	1.058260E+01	-8.537483E+00	1.359706E+01	1.949586E+00
4.055600E+02	4.513280E-01	-3.616830E-01	5.783697E-01	-6.757788E-01	1.107704E+01	-8.876884E+00	1.419506E+01	2.040075E+00
3.695300E+02	4.721900E-01	-3.756900E-01	6.034123E-01	-6.720725E-01	1.158906E+01	-9.220644E+00	1.480968E+01	2.135003E+00
3.367000E+02	4.941260E-01	-3.901740E-01	6.296001E-01	-6.688823E-01	1.212744E+01	-9.576128E+00	1.545242E+01	2.234187E+00
3.067900E+02	5.170740E-01	-4.051350E-01	6.568865E-01	-6.646077E-01	1.269066E+01	-9.943319E+00	1.612211E+01	2.344655E+00
2.795400E+02	5.410950E-01	-4.205720E-01	6.853208E-01	-6.607210E-01	1.328022E+01	-1.032219E+01	1.681998E+01	2.446557E+00
2.547000E+02	5.659500E-01	-4.361890E-01	7.145350E-01	-6.563306E-01	1.389024E+01	-1.070548E+01	1.753699E+01	2.558938E+00
2.320700E+02	5.919970E-01	-4.528820E-01	7.449963E-01	-6.523971E-01	1.452951E+01	-1.110047E+01	1.828461E+01	2.667100E+00
2.114600E+02	6.189980E-01	-4.685540E-01	7.763384E-01	-6.479378E-01	1.519221E+01	-1.149983E+01	1.905385E+01	2.793794E+00
1.926700E+02	6.470720E-01	-4.854820E-01	8.089468E-01	-6.436771E-01	1.588123E+01	-1.191528E+01	1.985416E+01	2.925731E+00
1.755500E+02	6.765760E-01	-5.027090E-01	8.428947E-01	-6.392184E-01	1.660536E+01	-1.233810E+01	2.068173E+01	3.059133E+00
1.599600E+02	7.070940E-01	-5.201730E-01	8.778165E-01	-6.342530E-01	1.735437E+01	-1.276672E+01	2.154445E+01	3.197120E+00
1.457500E+02	7.390420E-01	-5.377570E-01	9.139334E-01	-6.290269E-01	1.813847E+01	-1.319829E+01	2.243210E+01	3.341577E+00
1.328000E+02	7.721220E-01	-5.559960E-01	9.514746E-01	-6.240812E-01	1.895036E+01	-1.364593E+01	2.335225E+01	3.491143E+00
1.210000E+02	8.065740E-01	-5.743540E-01	9.901738E-01	-6.187946E-01	1.979593E+01	-1.409650E+01	2.430206E+01	3.646918E+00
1.102500E+02	8.420980E-01	-5.929510E-01	1.029913E+00	-6.134960E-01	2.067308E+01	-1.455299E+01	2.527737E+01	3.807539E+00
1.004600E+02	8.791720E-01	-6.117260E-01	1.071052E+00	-6.079002E-01	2.157771E+01	-1.501373E+01	2.628759E+01	3.975169E+00
9.153600E+01	9.177960E-01	-6.306210E-01	1.113567E+00	-6.020182E-01	2.252567E+01	-1.547747E+01	2.733053E+01	4.149807E+00
8.340500E+01	9.573740E-01	-6.495750E-01	1.156941E+00	-5.961479E-01	2.352670E+01	-1.594266E+01	2.839506E+01	4.328759E+00
7.599500E+01	9.986240E-01	-6.686490E-01	1.201808E+00	-5.900101E-01	2.459945E+01	-1.641080E+01	2.949625E+01	4.515270E+00
6.924400E+01	1.041300E+00	-6.880800E-01	1.248102E+00	-5.839227E-01	2.555686E+01	-1.688770E+01	3.063246E+01	4.708230E+00
6.309200E+01	1.085290E+00	-7.069150E-01	1.295216E+00	-5.773310E-01	2.663651E+01	-1.734997E+01	3.178876E+01	4.907130E+00